

# Long Time Confinement of Toroidal Electron Plasmas in Proto-RT

H. Saitoh\*, Z. Yoshida\*, H. Himura\*, J. Morikawa<sup>†</sup>, M. Fukao<sup>†</sup> and H. Wakabayashi\*

\*Graduate School of Frontier Sciences, The University of Tokyo, Bunkyo-ku, Tokyo 113-8656 Japan

<sup>†</sup>High Temperature Plasma Center, The University of Tokyo, Bunkyo-ku, Tokyo 113-8656 Japan

**Abstract.** Long-term confinement (the upper limit is set by the diffusion due to neutral collisions) of toroidal electron plasmas is achieved in a dipole magnetic field configuration of an internal conductor device by the optimization of internal potential profiles. The application of a negatively biased electrode makes possible the elimination of a potential well inside the plasma and results in the stabilization of the diocotron instability. In the experimental parameters of the magnetic field  $B \sim 100$  G and back pressure  $P \sim 10^{-4}$  Pa ( $\sim 10^{-6}$  Torr), the obtained maximum decay time of the trapped charge (number density  $n_e \sim 10^{12}$  m<sup>-3</sup>) is 200 msec, which is comparable to the classical neutral diffusion time. It is demonstrated that toroidal magnetic surface configurations have excellent confinement properties for non-neutral plasmas, and might be useful as applications for novel traps of charged particles such as anti-matters or other multi-fluid non-neutral plasmas.

## INTRODUCTION

Toroidal traps for non-neutral plasmas [1-3] are attracting renewed interest in spite of the long history of study regarding them. In toroidal geometry, we can simultaneously confine multiple species of charged particles at any degree of non-neutrality, because toroidal devices use no electrostatic potential well along the magnetic field lines. The confinement of anti-matter and its mixtures such as pure positron and electron-positron plasmas [1, 4], or the formation of fast  $\mathbf{E} \times \mathbf{B}$  drift flow due to the strong self electric fields and testing for the resultant high  $\beta$  equilibrium of two fluid non-neutral plasmas (Double Beltrami state) [2, 5] are the expected applications of toroidal non-neutral traps.

The experiments on toroidal non-neutral plasmas have been carried out in a pure toroidal magnetic field configuration [3] for several decades. In these devices, many interesting properties of toroidal electron plasmas, such as equilibria, confinement, and electrostatic fluctuation modes, etc., have been intensively investigated. Recently, the use of another magnetic field configuration for toroidal non-neutral plasmas has been proposed and these traps are expected to show different confinement properties for non-neutral plasmas. The trapping of non-neutral plasmas in a magnetic surface configuration is currently conducted or under design using stellarator [1] or internal conductor devices [2].

In this study, we report the experimental investigation of the confinement properties of torus electron plasmas in Proto-RT (Prototype-Ring Trap) [2] (Fig. 1). The use of magnetic surface (dipole) configuration and potential optimization has made possible the stabilization of diocotron instability, and long-term (i.e., comparable to the diffusion

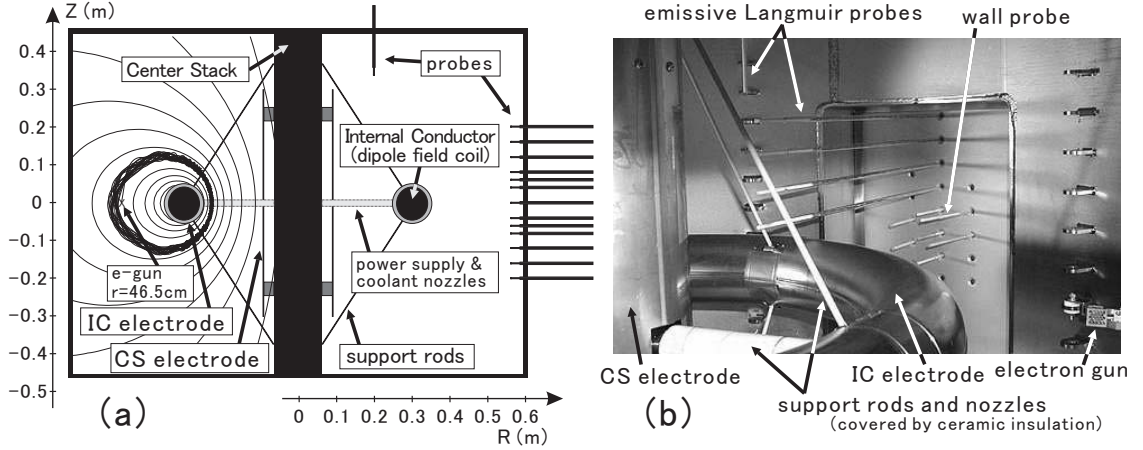


**FIGURE 1.** (a) The poloidal cross-section of Proto-RT, the dipole field magnetic surfaces, and the typical electron orbit. (b) Photographic view of experimental configurations inside Proto-RT. In order to suppress perturbations of the plasma, each probe was inserted independently while the other probes were located outside the confinement region.

time due to the neutral collisions) confinement of toroidal electron plasmas was demonstrated. The device setup, diagnostics, and recent results of pure electron experiments in Proto-RT will be described in the following sections.

## SETUP AND DIAGNOSTICS

Proto-RT is a normal conducting toroidal device constructed for investigating the relaxation states of two fluid flowing plasmas [5], the injection and confinement properties of non-neutral plasmas on magnetic surfaces [2], and the chaos-induced anomalous resistivity at the magnetic null line [6]. The chamber is drew to a base pressure of  $8 \times 10^{-5}$  Pa ( $\sim 6 \times 10^{-7}$  Torr) by a turbomolecular pump. Besides toroidal field coils, Proto-RT also has an internal conductor for a dipole magnetic field and a pair of vertical field coils, and the combination of these coils allows us to use a variety of magnetic field configurations. As an initial experiment, the trapping of electron plasmas on the magnetic surfaces of dipole magnetic field was carried out in this study. The coil current of the internal conductor is 10.5 kAt and the strength of the typical magnetic field is of the order of 0.01 T in the confinement region of the torus. For the optimization of the potential profiles of toroidal electron plasmas, two electrodes are installed in the confinement region of the Proto-RT vessel. In this experiment, we used a ring electrode on the internal conductor, and the effects of potential biasing up to 350V (DC, against the vessel wall) were examined, while the electrode on the center stack was shorted to the chamber. Electrons are injected by a LaB<sub>6</sub> cathode electron gun located at  $r = 46.5$  cm and  $z = 0$ . At an operating acceleration voltage of 300 V, applied between the cathode and anode grid located 2 mm behind the cathode, the electron beam current obtained was  $\sim 10$  mA. The circuit of the electron gun is operated by an FET high-speed semiconductor switch.

Internal potential distribution is measured using an array of emissive Langmuir

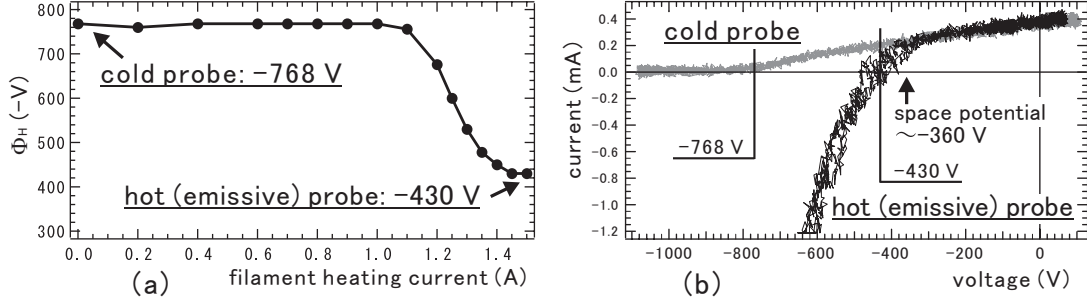


**FIGURE 2.** (a) Measured potentials ( $\Phi_H$ ) when the Langmuir probe tip is terminated by a high impedance ( $100\text{ M}\Omega$ ) voltage probe vs the heating current of the emissive Langmuir probe filament  $I_{\text{filament}}$ . When the tip is sufficiently heated,  $\Phi_H$  saturates to a certain value due to the space charge limit. (b) I-V curves of emissive ( $I_{\text{filament}} = 1.5\text{ A}$ ) and cold (non-emitting,  $I_{\text{filament}} = 0\text{ A}$ ) Langmuir probes.  $\Phi_H$  of the emissive probe gives a good approximation of the space potential, while  $\Phi_H$  of the cold probe is close to the sum of the potential and kinetic energy of the plasmas.

probes [7]. The probe tip is a thoria-tungsten spiral filament and is heated by the passage of a current. For the measurements of potential profiles, the tip is terminated across a high impedance ( $100\text{ M}\Omega$ ) voltage probe, in order to avoid perturbations to the plasma. When compared with the I-V characteristics of hot (emissive) and cold (non-emitting or usual) probes in Fig 2, the measured potential ( $\Phi_H$ ) gives a crossing point of the I-V curve and the load line of the high impedance. The floating potential of a sufficiently heated emissive probe is close to the space potential, and thus  $\Phi_H$  of the emissive probe gives a good approximation of the space potential of the electron plasmas. Although the charge of the escaping thermoelectrons of the emissive probes during the measurements of I-V curves (up to  $1\text{ mA}$ ) might be comparable to the confined electron charge, the I-V curves above the space potential show that the electron emission of the probe tip does not affect the electron density of the plasmas. This is possibly because the density limit is set by the acceleration voltage of the electron gun and further addition of electrons does not contribute to the plasma density.

For the measurements of electrostatic fluctuations and the remaining charge of electron plasmas, we have employed a wall probe [3]. As a wall tip, sensor foil (a copper sheet of  $5 \times 15\text{ mm}$ ) is installed in an insulating quartz tube and located just outside the confinement region in the chamber. The foil is grounded to the chamber via a current amplifier, and the detected image current indicates the oscillation in the plasmas. By integrating the escaping image current when the plasma is externally destroyed, the charge confinement time is also measured by wall probes.

## EXPERIMENTAL RESULTS

Non-neutral plasmas in a ring trap have a hollow distribution around the internal conductor. When  $V_{IC}$  is not externally controlled (i.e., the electrode is shorted to the chamber), the potential profile is also hollow, as shown in Fig. 3 (a1), resulting in a strong  $\mathbf{E} \times \mathbf{B}$  flow shear that may destabilize the diocotron instability. By applying a potential ( $V_{IC}$ )

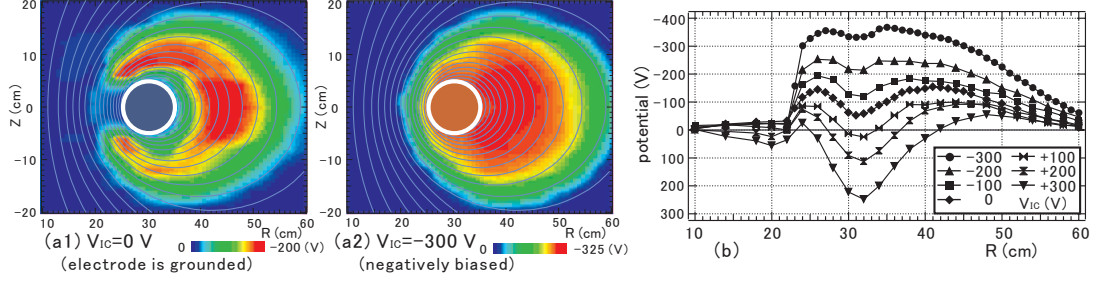


**FIGURE 3.** (a1) 2-d potential profiles of electron plasmas around the IC electrode, in the  $r$ - $z$  cross-section of the Proto-RT chamber, when the potential is not externally controlled (i.e., the IC electrode is shorted to the chamber) and (a2) when the IC electrode is negatively biased. Thin lines show the magnetic surfaces of the dipole field. The contour images are reconstructed from 284 data points taken shot by shot. (b) Radial potential profiles at  $z = +6$  cm while  $V_{IC}$  was varied from  $-300$  to  $+300$  V. The potentials in these figure are  $\Phi_H$  of the emissive Langmuir probes during the electron injection phase.

to the electrode, the potential distribution was successfully modified in the toroidal electron plasmas to form a stable equilibrium. The potential hole is eliminated using the negatively biased electrode, and in Fig. 3 (a2), potential contours surround the internal conductor. Fluctuations in the wall probe signal when  $V_{IC} = -300$  V are reduced by a factor of 10, in comparison with the fluctuation that occur when the electrode is grounded. After the electron injection was stopped, long-lasting oscillating signals indicating the confinement of electron plasmas were observed by controlling the bias voltage of the IC electrode.

An example of fluctuation and trapped charge, when the electrode is negatively biased, is shown in Fig. 4 (a). During the electron injection ( $t = -0.1$  to  $0$  msec), the observed dominant frequency was 510 kHz. After the electron injection was stopped, both the amplitude and frequency of the oscillation were damped, and a quiescent state followed. The first stable phase lasted for  $\sim 0.3$  msec, until the fluctuation grew rapidly. The amplitude decayed again, when the frequency dropped to 43 kHz. As shown in Fig. 4 (b), the fundamental frequencies at this period (i.e., just before the second quiescent phase) were proportional to  $E/B$ , where  $E$  is the strength of the external electric fields and  $B$  is the dipole magnetic field strength. These scalings and the observed frequency drop during the charge decay suggest that the observed fluctuations are due to diocotron oscillation. The second stable phase lasted relatively long ( $t^* \sim 200$  msec) and ended with a fast growth of fluctuation (a typical time constant was 0.1 msec), possibly caused by the ion resonance instability [9].

As shown in Fig. 5, the life time  $t^*$  of the electron cloud was scaled as  $\propto P^{-1}B^{2.5}$ , where  $P$  is the background neutral gas pressure and  $B$  is the dipole magnetic field strength, and both  $t^*$  and the decay time  $\tau_2$  of the trapped charge have a strong dependency on the strength of the magnetic field and the degree of vacuum. From the potential profiles in Fig. 3, the number density and the charge of the trapped electron cloud during the injection phase were calculated to be  $1 \times 10^{13} \text{ m}^{-3}$  (at peak) and  $3 \times 10^{-7}$  C, using the Poisson equation. The potential profiles after the electron injection was stopped were not obtained because of the perturbation problem of the Langmuir probes. However, judging from the frequency drop in the diocotron oscillation and also from the change of image

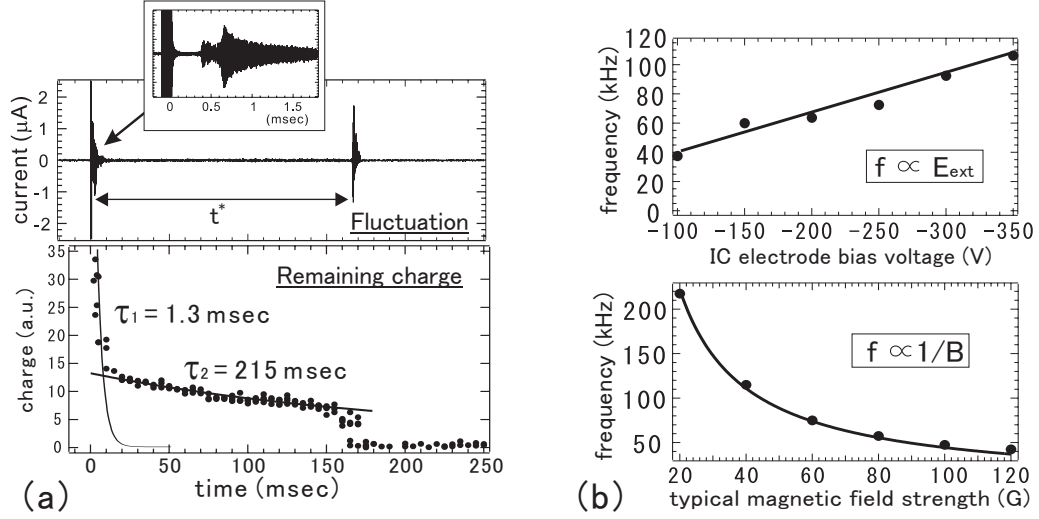


**FIGURE 4.** (a) Wall probe signal and decay of image charge on the wall foil. Electrons are injected to the chamber from  $t = -0.1$  to 0 msec. (b) Fundamental frequencies of electrostatic fluctuations just before the quiescent phase, as functions of the magnetic field strength  $B$  and the potential of the IC electrode  $V_{IC}$ .

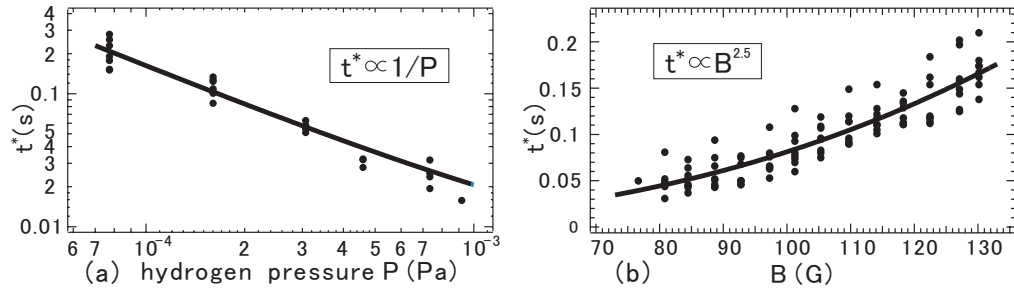


**FIGURE 5.** The life time  $t^*$  (stable confinement time before the sudden growth of instability) of electron plasmas as functions of (a) background pressure  $P$  and (b) typical magnetic field strength  $B$ .

charge on the wall probe, the peak number density and trapped charge of the remaining electrons in the quiet phase were estimated to be  $\sim 10^{12} \text{ m}^{-3}$  and  $\sim 10^{-8} \text{ C}$ , respectively.

In the current relatively high base pressure  $\sim 10^{-4} \text{ Pa}$  ( $\sim 10^{-6} \text{ Torr}$ ), neutral collisional effects are dominant in the diffusion process of electron plasmas. Using the experimental parameters of magnetic field strength  $B = 0.01 \text{ T}$ , electron number density  $n_e \sim 10^{12} \text{ m}^{-3}$ , and estimated electron temperature  $T_e \sim 1 \text{ eV}$  (which is close to the  $\mathbf{E} \times \mathbf{B}$  drift speed of electron plasmas), the classical diffusion time was  $t_D \sim v_{en}^{-1} \lambda_D^2 r_L^{-2} \sim 0.1 \text{ sec}$ . Both the decay time  $\tau_2$  and the life time  $t^*$  are comparable to  $t_D$ , suggesting that the current confinement time is set by the diffusion due to the electron-neutral collisions. Some preliminary experiments have also shown that the electrostatic fluctuations during the trap phase are stabilized by the effects of magnetic shear [8].

In conclusion, long-term confinement (comparable to the diffusion time due to neutral collisions) of toroidal electron plasmas was achieved in the dipole magnetic field configuration of an internal conductor device by controlling the internal potential distribution.

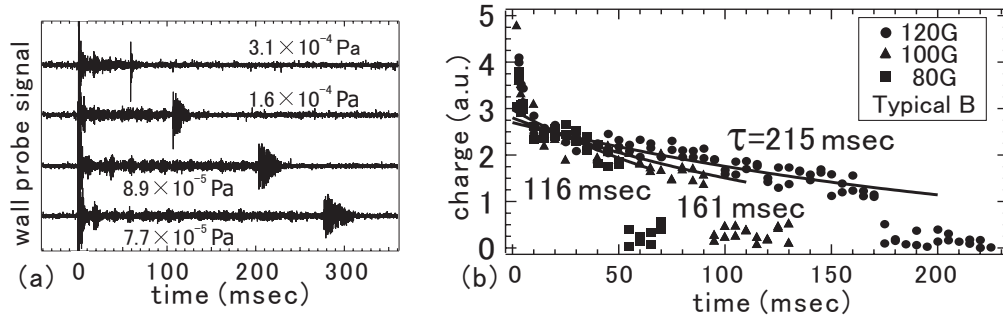


**FIGURE 6.** (a) Wave form of wall probe signals (electrostatic fluctuation of the plasma) in the variation of back pressure (hydrogen) and (b) decay of trapped charge on the wall probe in the variation of magnetic field strength. Electrons are injected from  $t = -0.1$  to 0 msec.

It was demonstrated that a magnetic surface configuration has excellent confinement properties for non-neutral plasmas, and that it might be usefully applied in novel traps of charged particles such as anti-matter or other multi-fluid non-neutral plasmas.

## ACKNOWLEDGMENTS

This work was supported by a Grant-in-Aid for Scientific Research (14102033) from MEXT Japan. The work of HS was supported in part by a JSPS Research Fellowship for Young Scientists.

## REFERENCES

1. T. S. Pedersen and A. H. Boozer, *Phys. Rev. Lett.* **88**, 205002 (2002); T. S. Pedersen, *Phys. Plasmas* **10**, 334 (2003); T. S. Pedersen *et al.*, *J. Phys. B: At. Mol. Opt. Phys.* **36**, 1029 (2003).
2. Z. Yoshida, Y. Ogawa, H. Himura *et al.*, in *Nonneutral Plasma Physics III and IV*, (AIP, New York); S. Kondoh and Z. Yoshida, *Nucl. Inst. and Meth. in Phys. Res. A* **382**, 561 (1996); C. Nakashima and Z. Yoshida, *Nucl. Inst. and Meth. in Phys. Res. A* **428**, 284 (1998); C. Nakashima *et al.*, *Phys. Rev. E* **65**, 036409 (2002); H. Saitoh, Z. Yoshida, and C. Nakashima, *Rev. Sci. Instrum.* **73**, 87 (2002).
3. J. D. Daugherty and R. H. Levy, *Phys. Fluids* **10**, 155 (1967); W. Clark *et al.*, *Phys. Rev. Lett.* **37**, 592 (1976); J. D. Daugherty *et al.*, *Phys. Fluids* **12**, 2677 (1969); L. Turner, *Phys. Fluids B* **3**, 1355 (1991); K. Avinash, *Phys. Fluids B* **3**, 3226 (1991); S. N. Bhattacharyya and K. Avinash, *Phys. Fluids B* **4**, 1702 (1992); P. Zaveri *et al.*, *Phys. Rev. Lett.* **68**, 3295 (1992); S. S. Khirwadkar *et al.*, *Phys. Rev. Lett.* **71**, 4334 (1993); M. R. Stoneking *et al.*, *Phys. Plasmas* **9**, 766 (2002).
4. C. M. Surko *et al.*, *Phys. Rev. Lett.* **62**, 901 (1989); M. Hori *et al.*, *Phys. Rev. Lett.* **89**, 093401 (2002); M. Amoretti *et al.*, *Nature* **419**, 456 (2002).
5. S. M. Mahajan and Z. Yoshida, *Phys. Rev. Lett.* **81**, 4863 (1998); Z. Yoshida and S. M. Mahajan, *Phys. Rev. Lett.* **88**, 095001 (2002).
6. T. Uchida, *Jpn. J. Appl. Phys.* **33**, L 43 (1994); Z. Yoshida *et al.*, *Phys. Rev. Lett.* **81**, 2458 (1998).
7. A. Tsushima, *Jpn. J. Appl. Phys.* **35**, 2820 (1996); H. Himura *et al.*, *Phys. Plasmas* **8**, 4651 (2001).
8. S. Kondoh, T. Tatsuno, and Z. Yoshida, *Phys. Plasmas* **8**, 2635 (2001).
9. R. H. Levy, J. D. Daugherty, and O. Buneman, *Phys. Fluids* **12**, 2616 (1969); J. Fajans, *Phys. Fluids B* **5**, 3127 (1993); A. J. Peurrung, J. Notte, and J. Fajans, *Phys. Rev. Lett.* **70**, 295 (1993).